C_4 anatomy can evolve via a single developmental change

Authors: Marjorie R. Lundgren[1,2] (m.lundgren@lancaster.ac.uk), Luke T. Dunning[1] (l.dunning@sheffield.ac.uk), Jill K. Olofsson[1] (j.k.olofsson@sheffield.ac.uk), Jose J. Moreno-Villena[1] (jjmorenovillena1@sheffield.ac.uk), Jacques W. Bouvier[1] (jbouvier1@sheffield.ac.uk), Tammy Sage[3] (tammy.sage@utoronto.ca), Roxana Khoshravesh[3] (r.khoshravesh@utoronto.ca), Stefanie Sultmanis[3] (stefanie.sultmanis@mail.utoronto.ca), Matt Stata[3] (matt.stata@mail.utoronto.ca), Brad Ripley[4] (b.ripley@ru.ac.za), Maria S. Vorontsova[5] (M.Vorontsova@kew.org), Guillaume Besnard[6] (guillaume.besnard@univ-tlse3.fr), Claire Adams[4] (claire3889@gmail.com), Nicholas Cuff[7] (Nicholas.Cuff@nt.gov.au), Anthony Mapaura[8] (mapaura@yahoo.com), Matheus Bianconi[1] (mebianconi1@sheffield.ac.uk), Christine M. Long[9] (christine.long@nt.gov.au), Pascal-Antoine Christin[1] (p.christin@sheffield.ac.uk), Colin P. Osborne[1]* (c.p.osborne@sheffield.ac.uk)

[1]Department of Animal and Plant Sciences, University of Sheffield, Western Bank, Sheffield S10 2TN, UK

[2]Current address: Lancaster Environment Centre, Lancaster University, Lancaster, LA1 4YQ, UK

[3]Department of Ecology and Evolutionary Biology, University of Toronto, 25 Willcocks Street, Toronto, Ontario M5S 3B2, Canada

[4]Botany Department, Rhodes University, Grahamstown 6139, South Africa

[5]Comparative Plant and Fungal Biology, Royal Botanic Gardens, Kew, Richmond, Surrey, TW9 3AB, UK

[6]Laboratoire Évolution & Diversité Biologique (EDB UMR5174), Université de Toulouse, CNRS, ENSFEA, UPS, IRD, 118 route de Narbonne, 31062 Toulouse, France

[7]Northern Territory Herbarium, Department of Environment and Natural Resources. PO Box 496, Palmerston, NT 0831, Australia

[8]National Herbarium and Botanic Garden, Harare, Zimbabwe

[9]Department of Primary Industry and Fisheries, Northern Territory Government, Darwin, NT 0801, Australia

*__Author for correspondence__: Colin P. Osborne; c.p.osborne@sheffield.ac.uk; Tel: +44-114-222-0146; Fax: +44-114-222-0002

Running title: One anatomical change key for C_4 emergence

Keywords: *Alloteropsis*, bundle sheath, C_3-C_4 intermediate, C_4 photosynthesis, evolution, grass, leaf anatomy, mesophyll, vein density

Article type: Letter

Words in the abstract: 148

Words in the main text: 4999

Number of references: 57

Number of figures: 4

Number of tables: 2

Number of text boxes: 0

Statement of authorship: MRL, PAC and CPO designed the study. MRL produced and analyzed the data, with the help of LTD, JJMV, and JWB. TS and RK performed the immunolocalisations and TEM imaging. SS assisted with immunolocalisation sample preparation. MS assisted with tissue fixation. MRL, LTD, JKO, BR, MSV, GB, CA, NC, AM, MB, CML, PAC, and CPO contributed plant material. MRL, PAC, and CPO interpreted the results and wrote the paper, with the help of all the authors.

Data accessibility statement: Should this manuscript be accepted, the data supporting the results will be archived in the public repository Dryad and the data DOI will be included at the end of the article.

Abbreviations: BS, bundle sheath; CCP, CO_2 compensation point, IS, inner sheath; LDA, linear discriminant analysis; M, mesophyll; OS, outer sheath

Abstract

C_4 photosynthesis is a complex trait that boosts productivity in warm environments. Paradoxically, it evolved independently in numerous plant lineages, despite requiring specialized leaf anatomy. The anatomical modifications underlying C_4 evolution have previously been evaluated through interspecific comparisons, which capture numerous changes besides those needed for C_4 functionality. Here, we quantify the anatomical changes accompanying the transition between non-C_4 and C_4 phenotypes by sampling widely across the continuum of leaf anatomical traits in the grass *Alloteropsis semialata*. Within this species, the only trait that is shared among and specific to C_4 individuals is an increase in vein density, driven specifically by minor vein development that yields multiple secondary effects facilitating C_4 function. For species with the necessary anatomical preconditions, developmental proliferation of veins can therefore be sufficient to produce a functional C_4 leaf anatomy, creating an evolutionary entry point to complex C_4 syndromes that can become more specialized.

INTRODUCTION

The vast majority of plants use C_3 photosynthesis, but some lineages evolved the C_4 pathway to overcome environmentally induced limitations on carbon fixation (Ehleringer *et al.* 1991; Sage *et al.* 2011). Net carbon fixation by C_3 photosynthesis is decreased in warm, high light, arid, and saline environments that lower CO_2 concentrations within the leaf and increase photorespiration, the process initiated when O_2 instead of CO_2 is fixed by the enzyme Rubisco (Chollet & Ogren 1975). To circumvent the losses of carbon and energy caused by photorespiration, the C_4 pathway spatially separates the initial fixation of carbon and its assimilation by Rubisco across two leaf compartments, thereby concentrating CO_2 at the enzyme's active site to promote CO_2- rather than O_2-fixation (Downton & Tregunna 1968; Hatch 1976). A number of anatomical and biochemical functions must work in concert to sustain the high fluxes of the C_4 cycle, and comparisons of average C_4 and C_3 plants suggest that the evolution of the C_4 phenotype required a large number and scale of changes (Hattersley 1984). Despite this apparent complexity, the C_4 trait evolved many times independently (Sage *et al.* 2011). Resolving this paradox requires the quantitative distinction of changes that were involved in the evolutionary transition from C_3 to C_4, from those that preceded or followed it.

In most C_4 plants, carbon fixation within leaf mesophyll tissue (M) is used to concentrate CO_2 and boost Rubisco activity within bundle sheath tissue (BS), whereas Rubisco in C_3 plants operates within the M where it depends on atmospheric CO_2 diffusion (Fig. 1; Brown 1975; Hattersley *et al.* 1977; Hatch 1987). Efficient C_4 leaves require large BS volumes to accommodate the necessary photosynthetic organelles, including chloroplasts containing abundant Rubisco, and a small distance between M and BS compartments to allow the rapid transfer of metabolites (Fig. 1; Hattersley & Watson 1975; Lundgren *et al.* 2014). These traits vary among C_3 plant lineages and, in grasses, C_4 photosynthesis evolved only within those groups with large fractions of BS (Christin *et al.* 2013; Lundgren *et al.* 2014). Comparisons of multiple C_4 lineages with their C_3 relatives indicate that the evolution of C_4 leaf anatomy involved ultrastructural rearrangements and further decreases to the relative volume of M compared to BS tissue (Hattersley 1984; Dengler *et al.* 1994; McKown &

Dengler 2007; Christin *et al.* 2013). These properties can be achieved via a variety of leaf structural modifications, allowing C_4 anatomy to be realized differently each time it evolved, in some cases involving the use of different tissue types for the C_4 BS function (Brown 1975; Soros and Dengler 2001; Christin *et al.* 2013; Freitag and Kadereit 2014; Lundgren *et al.* 2014). While the differences between a diverse range of C_3 and C_4 species are well known, the minimum set of leaf anatomical modifications required to carry out C_4 photosynthesis remains to be established.

The grass *Alloteropsis semialata* provides an outstanding system to capture the early events during C_4 evolution because it includes genetically divergent C_4 individuals, as well as a diversity of non-C_4 plants encompassing C_3 and C_3-C_4 intermediate phenotypes (Ellis 1974; Lundgren *et al.* 2016), which emerged in the paleotropics (Lundgren *et al.* 2015). The inner sheath (*i.e.*, the mestome sheath), which is present in all C_3 grasses, has been co-opted for the C_4 BS function in *A. semialata*. Previous studies have compared leaf properties among C_4 and non-C_4 leaves of a few *A. semialata* accessions (Ellis 1974; Frean *et al.* 1983; Ueno & Sentoku 2006; Lundgren *et al.* 2016; Dunning *et al.* 2017), but a broader sampling is required to establish which properties are unique to each photosynthetic type.

The primary focus of this study is to compare leaf anatomy in accessions spanning the diversity of each photosynthetic type to distinguish the structural diversifications that occurred before, during, and after C_4 emergence in this species. We hypothesize that the properties that predate C_4 evolution will be shared by at least some of the non-C_4 individuals, while those that happened after C_4 evolution in a phase of subsequent adaptation will be restricted to a subset of the C_4 populations. Properties unique to, and common among all, C_4 accessions represent those that were involved in the initial transition to a C_4 physiology. We conducted a large scan of the diversity within the species using traits linked to the number and size of different cell types, and used controlled growth experiments to verify that anatomical differences are not environmentally induced. This evaluation of the gross leaf morphology was accompanied by a focused study in some individuals to identify ultrastructural changes that may also differ between C_4 and non-C_4 accessions. Overall, our work

shows that a complex trait of large ecological significance can evolve via a few key developmental changes.

MATERIALS AND METHODS

Characterizing photosynthetic types

Photosynthetic type was determined by a combination of stable isotope and CO_2 compensation point (CCP) data (Table S1; Dataset S1), as previously described (Lundgren *et al.* 2016). The carbon isotope composition of plant tissues ($\delta^{13}C$) distinguishes photosynthetic types (von Caemmerer *et al.* 2014), such that plants with $\delta^{13}C$ values higher than -17‰ were considered to have a fully functioning C_4 system, while those with values lower than this threshold were considered either C_3 or C_3-C_4. CCPs were used to distinguish C_3-C_4 from C_3 plants, and to support the $\delta^{13}C$ results. The CCP indicates the CO_2 concentration within the leaf at which CO_2 assimilation via photosynthesis equals CO_2 loss via photorespiration and respiration. Because less CO_2 is ultimately lost to photorespiration in C_3-C_4 plants, they have very low CCPs compared to C_3 plants. Thus, non-C_4 plants with CCPs greater than or equal to 35 μmol mol^{-1} were classified as C_3, while those less than 35 μmol mol^{-1} were classified as C_3-C_4. CCPs were calculated on 27 living accessions (6 C_3, 4 C_3-C_4, and 17 C_4), following published protocols (Bellasio *et al.* 2016a,b; Lundgren *et al.* 2016). Non-C_4 accessions for which live material was unavailable were assumed to have the same photosynthetic type as their closest relatives, as identified by phylogenetic relationships (Table S1).

Leaf samples

Fifty *Alloteropsis semialata* (R.Br.) Hitchc. accessions distributed across the species' geographic range, including 17 C_3, 6 C_3-C_4, and 27 C_4, were used to assess intraspecific anatomical variation. Leaf samples from 44 of the 50 accessions were collected from their original field site and preserved until embedding was possible. For the remaining six accessions, leaf samples were taken from plants grown under controlled environment conditions as in Lundgren *et al.* (2016). For all samples, leaf

pieces 3-5 mm in length were embedded in methacrylate embedding resin (Technovit 7100, Heraeus Kulzer GmbH, Wehrhein, Germany), sectioned 6-8 μm thick on a manual rotary microtome (Leica Biosystems, Newcastle, UK), and stained with Toluidine Blue O (Sigma-Aldrich, St. Louis, MO, USA). Stained leaf sections were imaged using microscopy-imaging software with a camera mounted on a microscope (Cell A, Olympus DP71, and Olympus BX51, respectively; Olympus, Hamburg, Germany) and the images were stitched together using DoubleTake (v2.2.9, Echo One, Frederikssund, Denmark).

Leaf anatomy measurements

Anatomical traits were measured using ImageJ (Fig. S1; Schneider *et al.* 2012) from the cross-section of a single leaf segment from the centre of the leaf blade, avoiding segments immediately adjacent to the midrib and lateral edges of the cross-section. Vein orders were distinguished following Renvoize (1987). A single segment was defined as the leaf area falling between two secondary veins, which are large veins with metaxylem. Tertiary and minor veins (*e.g.*, quaternary and quinary orders) lack metaxylem. In this species, the extraxylary fibres that flank both the adaxial and abaxial edges of tertiary veins distinguish them from higher order minor veins, which can be flanked by fibres on one side only (Fig. S1).

The cross-sectional area of the whole segment, combining M, BS, epidermis and bulliform cells, extraxylary fibres, and BS extensions, as well as any transverse veins or tear spaces was measured. For all accessions, the total BS (*i.e.*, the mestome sheath; the compartment used for the Calvin cycle in C_4 *A. semialata*), outer sheath, and vein areas were measured separately for secondary, tertiary, and any minor veins. The area of M tissue was calculated as the total area remaining after accounting for all other tissue types. In addition, the cross-sectional area of individual M and BS cells (hereafter 'size') was measured (Fig. S1). Although the depth of individual cells can vary, it is their cross-sectional areas, and not their three-dimensional volumes, that primarily influence the proportion of each tissue in the leaf.

Linear discriminant analysis

We used a Linear Discriminant Analysis (LDA) to explain the variation between photosynthetic types (*i.e.*, the test maximizes between-group variance while minimising within-group variance). We performed the LDA on the 50 accessions with leave-one-out cross-validation and then bootstrapping over 100 runs, using the MASS package in R (Venables & Ripley 2002). Prior probabilities were based on the relative sample size of the categorical variable (*i.e.*, 0.34, 0.12, and 0.54 for C_3, C_3-C_4, and C_4 groups, respectively). We chose predictor variables that were likely to influence the M:BS ratio, including the number of M cells between major veins, average size of individual M cells, number of minor veins per segment, leaf thickness, and the average size of BS cells on tertiary veins.

To test the generality of our findings from *A. semialata*, we carried out an equivalent LDA for a larger sample of 157 grasses including one C_3 and one C_4 *A. semialata* and representing 17 independent C_4 lineages. Predictor variables in this analysis were based on the anatomical measurements of Christin *et al*. (2013) and chosen to best match the variables used in the *A. semialata* LDA described above, including the number of mesophyll cells between veins, mesophyll cell width, proportion of veins that are minor, leaf thickness, inner BS cell width, and outer BS cell width. The species were grouped as C_3, C_4 species using the inner BS, and C_4 species using the outer BS.

Vein order analysis

To determine whether the pattern of vein density observed in the main dataset was maintained across a larger sample, we counted the total number of veins per segment and the presence or absence of minor veins in 91 additional accessions consisting of herbarium specimens that had been rehydrated in distilled water overnight at 4°C prior to embedding, sectioning, staining, and imaging as described above. Together with the 50 previous samples, this larger dataset included a total of 72 C_4 (*i.e.*, $\delta^{13}C >$ -17‰) and 69 non-C_4 (*i.e.*, $\delta^{13}C <$ -17‰) accessions distributed across the species' geographic range.

206 **Ultrastructure and immunohistochemistry**

207 To investigate whether ultrastructural changes might also differ between photosynthetic types within
208 this species, we analysed the spatial distributions of organelles and enzymes in one population
209 representing each of the C_3, C_3-C_4, and C_4 types. Recently expanded mature leaf tissue was prepared
210 for transmission electron microscopy and processed for immunodetection of the large subunit of
211 Rubisco (RBCL) and glycine decarboxylase H subunit (GLDH) as previously described (see
212 Supporting Information Materials 1; Khoshravesh *et al.* 2017).

213

214 **Leaf anatomy in a common environment**

215 To determine the degree to which the various leaf anatomical phenotypes arose from plastic
216 development responses to their differing native growth environments, we compared field phenotypes
217 to those obtained from live tillers of 17 *A. semialata* accessions (5 C_3, 4 C_3-C_4, and 8 C_4) after growing
218 for a minimum of three months in a common growth chamber, with conditions as described in
219 Lundgren *et al.* 2016. The environmental conditions (Fick & Hijmans 2017) at the field collection
220 sites are detailed in Table S2. On both field and controlled environment samples, the number and
221 order of veins, minimum number of M cells separating veins, area of inner BS cells, segment length
222 and thickness, and IVD were determined on one segment per leaf.

223

224 **Plasticity for leaf anatomy in response to low CO_2**

225 To further test whether C_4-compatible phenotypes could emerge from plastic responses to the
226 environment, as previously suggested (Li *et al*., 2014), we carried out a CO_2 manipulation experiment
227 designed to promote photorespiration. One C_4 (MDG, South Africa) and one C_3 (GMT, South Africa)
228 plant were initially grown from seed in a controlled environment chamber set as described in
229 Lundgren *et al.* 2016, but with 400 μmol mol^{-1} CO_2 concentration. Both plants were split into five
230 replicate cuttings and kept in the same growth chamber conditions to re-establish for four months.
231 From each replicated clone, one fully expanded, mature leaf was sampled and fixed in 4:1

ethanol:acetic acid solution. The growth chamber was then set to 180 μmol mol^{-1} CO_2 concentration for the next four months to promote photorespiration, while maintaining the other environmental conditions, and one new fully expanded leaf was again sampled and fixed. All leaf samples from the 400 (*i.e.*, ambient) and 180 (*i.e.*, low) CO_2 treatments were embedded, sectioned, and imaged as described above. To determine whether the plants used different photosynthetic pathways in the two CO_2 growth environments, we determined CCP and carboxylation efficiency, as described in Lundgren *et al*. (2016).

RESULTS

Alloteropsis semialata presents a continuum of leaf anatomy

The ratio of M to BS tissue, a trait known to differ among C_3 and C_4 species (Hattersley 1984), forms a continuum within *Alloteropsis semialata*, along which photosynthetic types are sorted (Fig. 2). Indeed, the smallest values are restricted to C_4 accessions and the largest are found in C_3 individuals. When considering the area in cross-section between two secondary veins (*i.e.*, a leaf segment from here onward; Fig. S1), the M area is over ten times larger than the BS area in C_3 accessions, but less than five times larger in C_4 accessions (Dataset S1). As expected, C_3-C_4 accessions are intermediate in their overall leaf anatomy, with five to ten times more M than BS. These M:BS ranges are consistent with those measured in other C_3 and C_4 grasses (Christin *et al.* 2013).

C_3, C_3-C_4, and C_4 *Alloteropsis semialata* have distinct leaf anatomy

Variation in M:BS ratios can arise via changes to several underlying traits (Lundgren *et al.* 2014). Our modelling shows that M area is the product of leaf thickness and interveinal distance (IVD; Table 1). The latter is predicted by the number and size of M cells between veins (Table 1). BS area is explained by the number of BS units (*i.e.*, the number of veins per segment) and the size of BS cells (Table 1). When these potential explanatory traits are incorporated within an LDA, all variance

between the three photosynthetic types is captured (Fig. 3a). In a bootstrapped sample, the mean overall predictive accuracy is 0.986, which is statistically indistinguishable from 1.0 (95% CI = 0.966 – 1.000). The mean predictive accuracy for C_4 (0.999, 95% CI = 0.995 – 1.000), C_3 (0.976, 95% CI = 0.918 – 1.000) and C_3-C_4 (0.926, 95% CI = 0.805 – 1.000) accessions are also statistically indistinguishable from 1.0. The analysis therefore confirms that leaf anatomy varies among photosynthetic types in a statistically predictable manner.

The first axis of the LDA explains 97.37% of the variance between photosynthetic types and clearly distinguishes C_4 from non-C_4 accessions (Fig. 3a). This axis is most strongly associated with the number of minor veins per segment, which were absent from all non-C_4 accessions in this analysis (Table 2). The second axis explains 2.63% of the variance between groups, clearly distinguishes C_3 from C_3-C_4 plants, and is most strongly associated with the number of M cells between major veins (*i.e.*, secondary and tertiary order veins) and the number of minor veins (Fig. 3a; Table 2). Since minor veins are restricted to C_4 individuals, their contribution to LD2 is linked to diversity within the C_4 group. These results indicate that most of the variance in the dataset stems from the contrast between C_4 and non-C_4 individuals, and is driven entirely by a single underlying trait, the presence of minor veins. The phenotypic distance between C_3 and C_3-C_4 individuals is very small, being explained by the number of M cells between major veins. Conversely, leaf thickness and the cross-sectional areas of individual BS and M cells poorly distinguish photosynthetic types in this species.

The first two axes of an LDA of anatomical traits on the larger species dataset explain 89.62% and 10.38% of the variation, respectively. The first axis clearly distinguishes C_4 species that use the inner bundle sheath from C_4 species using the outer sheath and the C_3 species (Fig. 3b), and is mostly associated with the proportion of minor veins, while the remaining anatomical traits are weakly correlated with both axes (Table 2).

Differences between C_4 and non-C_4 phenotypes arise from the development of minor veins

In *A. semialata*, the presence of minor veins is the only variable consistently distinguishing C_4 and

non-C_4 accessions. When the M:BS ratio is calculated in the absence of minor veins, the clear distinction between C_3-C_4 and C_4 accessions disappears, with nearly half the C_4 accessions overlapping with C_3-C_4 plants (Fig. 2). This shows that the development of minor veins in C_4 accessions reduces the M:BS ratio by increasing BS area and displacing M area. To confirm the restriction of minor veins to C_4 individuals, we screened vein architecture in a larger dataset (Fig. 4a,b; Dataset S2). Minor veins were present in all C_4 accessions and absent in all but five non-C_4 accessions. Four of these had only occasional and irregularly spaced minor veins, while the final accession is an individual originating from a natural cross between C_3-C_4 and C_4 individuals (Olofsson *et al.* 2016). Our data therefore show that the presence of frequent and regularly spaced minor veins is universally and uniquely associated with the C_4 genomic background, captures nearly all of the anatomical variation between C_4 and non-C_4 phenotypes, and explains overall differences in relative M and BS areas.

The proliferation of minor veins explains a number of patterns associated with C_4 anatomy. As expected, the number of M cells between consecutive veins differs among photosynthetic types, being the smallest in C_4 accessions (1-3), compared to C_3-C_4 (3-6) and C_3 (5-11) plants (Fig. S2). However, the number of M cells between major veins overlaps between the C_4 and non-C_4 groups (Fig. 4c), which indicates that the reduced distance between any pair of M and BS cells in C_4 accessions is caused by the differentiation of ground meristem cells into minor veins rather than a reduced proliferation of M cells. The high vein density of C_4 plants following the development of minor veins is accompanied by more than a twofold increase in extraxylary fibres (*i.e.*, tissue area per segment length) than is found in non-C_4 accessions (Fig. S3). Because the area of extraxylary fibres per vein does not differ between the photosynthetic types (Fig. S3), the increased fibre area in C_4 plants derives entirely from their greater vein density.

Other anatomical changes happened before or after the transition from C_3-C_4 to C_4 physiology

The development of minor veins explains the overall anatomical difference between C_4 and non-C_4

accessions, and is therefore linked to the emergence of a fully functioning C_4 physiology from a C_3-C_4 intermediate state. Evolutionary changes that happened once this C_4 physiology was in place would be restricted to some, but not all, C_4 individuals. In our dataset, such changes include further reductions to the M:BS ratio, potentially achieved via contractions to M airspace (Byott 1976) or increases in BS cell size. Indeed, although BS cell sizes of different photosynthetic types overlap, large increases to BS cell size characterize some African C_4 accessions (Figs S4-S5). The BS cell enlargement was therefore involved in the adaptation of C_4 physiology after it had emerged, possibly to accommodate more or larger organelles for a more efficient C_4 cycle, rather than being involved in its origin. Occasional hybridization between C_4 and non-C_4 individuals could affect the distribution of trait values, however non-C_4 *A. semialata* individuals are restricted to Africa, so that hybridization outside of Africa is unlikely. Yet, Asia and Australian accessions exhibit some of the smallest BS cells among C_4 accessions (Fig. S5).

Some characters observed in C_4 accessions are also present in C_3-C_4 individuals, but not C_3 ones, indicating that they are not associated with the transition to fully functional C_4 physiology, but might have facilitated it. These include a small increase in BS cell sizes in C_3-C_4 compared with C_3 plants and a decrease in outer sheath cell size, with C_3-C_4 accessions bridging the anatomical gap between C_3 and C_4 outer sheath cell sizes (Fig. 4c-d). This reduced outer sheath in C_3-C_4 and C_4 *A. semialata* likely facilitates metabolite exchanges between M and BS cells.

Differences between C_4 and non-C_4 leaves are not environmentally induced

Alloteropsis semialata plants grow naturally in diverse environments, depending on their photosynthetic background and evolutionary history (Lundgren *et al.* 2015). To verify that the differences we observe among photosynthetic types are not induced by environmental variations, we compared the leaves of field-collected plants after transplanting and growing them in a common controlled environment growth chamber for at least three months (Dataset S3; Fig. S6). Compared to field conditions, C_3 accessions produced more M cells between veins (p = 0.044) in the common

environment. Moreover, C_3-C_4 plants produced thicker leaves ($p = 0.040$), such that leaf thickness of the three photosynthetic types converged in the common environment, which is likely a result of the non-limiting light, nutrients, and water available in these conditions. However, the other traits were not influenced by growth conditions and leaf anatomy of the three photosynthetic types remained distinct when grown in the common environment.

We further verified that historical changes in atmosphere composition did not influence the leaf phenotype by comparing C_3 and C_4 *A. semialata* under current ambient (400 ppm) and the Pleistocene minimum (180 ppm) CO_2 concentrations. Plants grown under the low CO_2 concentration experience elevated photorespiration rates, which might have induced a more C_4-like anatomy. However, we found that plants did not shift photosynthetic state under the differing CO_2 conditions (*i.e.*, mean CCPs in ambient/low CO_2 for C_3 = 49.8/53.1 and C_4 = 4.6/8.1 µmol mol^{-1}; Dataset S4). Both C_3 and C_4 plants produced thinner leaves in the low CO_2 environment ($p = 0.0049$ C_3 / 0.0065 C_4), and C_4 plants developed smaller BS cells ($p = 0.011$; Fig. S6), probably because the lower carbon supply restricted development (Ripley *et al.* 2013). Importantly, the C_3 plants did not produce more veins (or any minor veins), larger BS cells, or fewer M cells between veins when grown under this high photorespiration condition. These results show that, even when photorespiration is high, a C_4-like phenotype is not plastically induced in C_3 *A. semialata*.

DISCUSSION

Photosynthetic types form a continuum, along which multiple biochemical, anatomical, and ultrastructural alterations increase the proportion of CO_2 fixed via the C_4 cycle. The emerging model of C_4 evolution involves gradual and overlapping phenotypic changes (Heckmann *et al*., 2013; Sage *et al*., 2014; Bräutigam & Gowik, 2016; Schlüter & Weber, 2016; Dunning *et al*., 2017), with traits acquired in differing orders among C_4 lineages (Williams *et al*., 2013). Different traits may be involved in the initial transition to a C_4 phenotype, and the subsequent adaptation and diversification

of that phenotype (Christin & Osborne, 2014; Watcharamongkol *et al*., 2018). Within the grass *Alloteropsis semialata*, we have shown that the only gross leaf property distinguishing all C_4 from all non-C_4 phenotypes is the development of frequent minor veins. The presence of these minor veins has multiple consequences, including an overall increase of vein density, enlargement of the total volumes of BS tissue, and a displacement of M tissue. These anatomical changes combine to facilitate C_4 cycle activity, as demonstrated by a strong correlation between leaf vein frequency and carbon isotope composition observed for this species (Lundgren *et al*., 2016). Our analyses of leaf ultrastructure indicate that the evolution of C_4 photosynthesis in *A. semialata* may have involved additional changes in organelle distribution among cell types (Supporting Information Materials 1; Figs S7-9), although the small sample of populations prevents us from differentiating ultrastructural changes linked to the transition to C_4 from those that happened later.

The change in venation inferred during the evolution of C_4 photosynthesis in *A. semialata* may have a number of physiological and ecological consequences. First, the increase in vein frequency is accompanied by an enhancement of unpigmented extraxylary fibres, which improves light transmission to the BS, and thus ATP production in these cells, facilitating photosynthetic carbon reduction (Bellasio & Lundgren 2016). Enhanced fibre density may also increase leaf toughness, reduce digestibility, and consequently deter herbivores (Caswell *et al.* 1973; Wilson *et al.* 1983). Secondly, the insertion of additional veins may influence leaf hydraulics. Model simulations for other plant species demonstrate that an increase in minor vein density can lead to greater leaf hydraulic conductance (McKown *et al*., 2010). However, empirical studies show that this is unlikely to improve drought tolerance, since the decline in hydraulic conductance during drought arises primarily outside veins (Scoffoni & Sack, 2017; Scoffoni *et al*., 2017a), while embolisms arise first in the midrib, not minor veins (Scoffoni *et al*., 2017b).

Our results complement those from previous comparisons among species, which show that an additional order of minor veins develops during the evolutionary transition from non-C_4 to C_4 forms of *Flaveria* (McKown & Dengler, 2009), while BS cell size is large in both C_3 and C_4 *Flaveria* species

(Kümpers *et al*., 2017). Our further analysis of leaf gross anatomy across multiple grass species shows that the insertion of additional minor veins is a frequent developmental mechanism for decreasing the M:BS ratio in those C_4 grasses that primarily localise Rubisco within the mestome sheath. The insertion of minor veins could occur via relatively few developmental changes, likely underpinned by changes to auxin, brassinosteroids, SHORTROOT/SCARECROW, and/or INDETERMINATE DOMAIN transcription factors (Kumar & Kellogg 2018; Sedelnikova *et al.* 2018). In grasses, vein orders develop sequentially as leaves grow wider, such that minor veins are initiated considerably later than other vein orders, usually once the leaf ceases to widen (Nelson & Langdale 1989; Sedelnikova *et al.* 2018). Thus, the development of functional minor veins likely arises via the heterochronic regulation of the existing machinery for vein formation, sustaining vein differentiation beyond that of non-C_4 plants (Nelson 2011; Sedelnikova *et al.* 2018), probably through the prolonged production of auxin during later phases of leaf elongation (Scarpella *et al.* 2010). Alternatively, minor veins may also result from a heterotopic specialization of auxin maxima that permits them to form closer together (Kumar & Kellogg 2018).

The possibility that a transition from non-C_4 to C_4 states can be caused by a single developmental alteration is a plausible explanation for the recurrent origins of C_4 leaf anatomy, and helps to resolve the paradox of how this complex trait emerged so many times. We also show that organelle number and size differs among photosynthetic types of *A. semialata*, but, here too, recent work indicates that one gene can control multiple ultrastructural modifications (Wang *et al.* 2017). Finally, transcriptome comparisons show that few genes encoding enzymes are upregulated during the transition from non-C_4 to C_4 in *A. semialata* (Dunning *et al.* 2017). We therefore conclude that the overall transition from a non-C_4 state to the form of C_4 photosynthesis observed in *A. semialata* involved relatively few genetic mutations.

The limited number of changes involved in the emergence of C_4 anatomy in *A. semialata* is partially explained by the presence of relatively enlarged BS in the C_3-C_4 accessions, since C_3 *A. semialata* BS size is similar to C_3 species from other grass lineages (Lundgren *et al*., 2014; 2016;

Dunning *et al.* 2017). The C_3 *A. semialata* phenotype might represent an evolutionary reversal from a C_3-C_4 state (Dunning *et al.* 2017), such that its leaf anatomy derives from an ancestral C_3-C_4 intermediate form. C_3-C_4 *A. semialata* are characterised by fewer M cell compared to C_3 accessions, and higher BS organelle abundance (Figs 3a, 4c and S7-9). These properties that had been selected for the C_3-C_4 physiology eased the subsequent transition to a full C_4 state, but it is important to note that the physiology and anatomy of C_3-C_4 *A. semialata* are typical for C_3-C_4 plants in general (Lundgren *et al.*, 2016), and their anatomical characteristics can be found among C_3 grasses (Hattersley 1984; Christin *et al.* 2013; Lundgren *et al.* 2014). The background against which C_4 anatomy evolved in *A. semialata* is therefore not exceptional.

Our conclusion that C_4 leaf anatomy can arise from one key developmental modification is apparently incompatible with the great anatomical specialization of other C_4 lineages, as well as the large phenotypic gaps separating them from their closest C_3 relatives (Dengler *et al.* 1994; Christin *et al.* 2013). However, most C_3 and C_4 sister lineages are separated by long periods of evolution, and comparing these groups therefore captures all of the changes that happened after the origin of C_4 photosynthesis to improve the efficiency of C_4 physiology and adapt it to various organismal and ecological contexts (Christin & Osborne 2014). Indeed, photosynthetic efficiency may be significantly lower in C_4 *A. semialata* than in species from some older C_4 lineages (Lundgren *et al*., 2016; Bräutigam *et al*., 2018). This suggests that C_4 photosynthesis in *A. semialata* may represent a rudimentary version of the physiological trait (Ueno & Sentoku 2006). The biochemical characteristics of the C_4 cycle in *A. semialata* may be one reason for this (Bräutigam *et al*., 2018), and the presence of Rubisco protein in M could be another (Ueno & Sentoku, 2006). Anatomical diversity may also explain some of the variation in physiological efficiency among *A. semialata* populations (Lundgren *et al.* 2016). Indeed, in *A. semialata*, enlargements of the BS cells beyond those seen in non-C_4 individuals are restricted to a subset of C_4 populations (Fig. 2) and thus happened after the emergence of C_4 physiology. Over time, accumulated modifications will move C_4 leaf anatomy far beyond that realized via a single developmental change. However, the fact that an initial

C_4 phenotype and the associated physiology can be accessed via a single modification likely placed multiple groups on a selective highway to highly specialized and successful variants of the C_4 syndrome.

ACKNOWLEDGEMENTS

This work was funded by a University of Sheffield Prize Scholarship to MRL, an ERC grant (grant number ERC-2014-STG-638333) and a Royal Society Research Grant (grant number RG130448). LTD and JKO are supported by a NERC grant (grant number NE/M00208X/1) and PAC is supported by a Royal Society University Research Fellowship (grant number URF120119). JWB was supported by 301 and Think Ahead Sheffield Undergraduate Research Experience grants to MRL. The work on ultrastructure was supported by a Natural Sciences and Engineering Research Council of Canada grant (no 2015-04878) to TLS. The authors thank Peter Westhoff, Stefanie Schulze, and Udo Gowik for use of their GLDH antibody, Susanne von Caemmerer for advice about outer bundle sheath cell resistance, Paul Hattersley for leaf samples and ^{13}C isotope data, John Thompson for field assistance and sample collection, Emma Jardine for discussion of linear discriminant analysis, Heather Walker for mass spectrometry assistance, Gareth Fraser for the use of his vibratome, and Emanuela Samaritani for histology assistance. Herbarium leaf samples were obtained from Kew Herbarium at the Royal Botanic Garden, the National Herbarium of South Africa in Pretoria, and National Museums of Kenya in Nairobi, and the National Botanic Garden of Belgium, Brussels, with the assistance of Martin Xanthos, Lyn Fish, Caroline Mashau, and Itambo Malombe.

REFERENCES

Bellasio, C. & Lundgren, M.R. (2016). Anatomical constraints to C_4 evolution: light harvesting capacity in the bundle sheath. *New Phytol.*, 212, 485-496.

Bellasio, C., Beerling, D.J. & Griffiths, H. (2016a). An Excel tool for deriving key photosynthetic parameters from combined gas exchange and chlorophyll fluorescence: theory and practice. *Plant Cell Environ.*, 39, 1180-1197.

Bellasio, C., Beerling, D.J. & Griffiths, H. (2016b). Deriving C_4 photosynthetic parameters from combined gas exchange and chlorophyll fluorescence using an Excel tool: theory and practice. *Plant Cell Environ.*, 39, 1164-1179.

Bräutigam, A. & Gowik, U. (2016) Photorespiration connects C_3 and C_4 photosynthesis. *J. Exp. Bot*., 67, 2953-2962.

Brautigam, A., Schluter, U., Lundgren, M.R., Flachbart, S., Ebenhoh, O., Schonknecht, G., Christin, P.A., Bleuler, S., Droz, J.M., Osborne, C. & Weber, A. (2018). Biochemical mechanisms driving rapid fluxes in C_4 photosynthesis. *bioRxiv*, p.387431.

Brown, W.V. (1975). Variations in anatomy, associations, and origins of Kranz tissue. *Am. J. Bot.*, 62, 395-402.

Byott, G.S. (1976). Leaf air space systems in C_3 and C_4 species. *New Phytol.*, 76, 295-299.

Caswell, H., Reed F, Stephenson S. N. & Werner P.A. (1973). Photosynthetic pathways and selective herbivory: a hypothesis. *Am. Nat.*, 107, 465-480.

Christin, P.A. & Osborne, C.P. (2014). The evolutionary ecology of C_4 plants. *New Phytologist*, 204, 765-781.

Christin, P.A., Osborne, C.P., Chatelet, D.S., Columbus, J.T., Besnard, G., Hodkinson, T.R., *et al.* (2013). Anatomical enablers and the evolution of C_4 photosynthesis in grasses. *Proc. Natl. Acad. Sci.*, 110, 1381-1386.

Chollet, R. & Ogren W.L. (1975). Regulation of photorespiration in C_3 and C_4 species. *Bot. Rev.*, 41, 137-179.

Dengler, N.G., Dengler, R.E., Donnelly, P.M. & Hattersley, P.W. (1994). Quantitative leaf anatomy of C_3 and C_4 grasses (Poaceae): bundle sheath and mesophyll surface area relationships. *Ann. Bot.*, 73, 241-255.

Downton, W.J.S. & Tregunna, E.B. (1968). Carbon dioxide compensation-its relation to photosynthetic carboxylation reactions, systematics of the Gramineae, and leaf anatomy. *Can. J. Bot.*, 46, 207-215.

Dunning, L.T., Lundgren M.R., Moreno- Villena J.J., Namaganda M., Edwards E.J., Nosil P., *et al.* (2017). Introgression and repeated co-option facilitated the recurrent emergence of C_4 photosynthesis among close relatives. *Evolution* 71, 1541-1555.

Ehleringer, J.R., Sage, R.F., Flanagan, L.B. & Pearcy R.W. (1991). Climate change and the evolution of C_4 photosynthesis. *Trends Ecol. Evol.*, 6, 95-99.

Ellis, R.P. (1974). The significance of the occurrence of both Kranz and non-Kranz leaf anatomy in the grass species *Alloteropsis semialata*. *S. Afr. J. Sci*., 70, 169-173.

Fick, S.E. & R.J. Hijmans. (2017). Worldclim 2: new 1-km spatial resolution climate surfaces for global land areas. *Int. J. Climatol*., 37, 4302-4315.

Frean, M.L., Ariovich, D. & Cresswell, C.F. (1983). C_3 and C_4 Photosynthetic and anatomical forms of *Alloteropsis semialata* (R. Br.) Hitchcock: 2. A comparative investigation of leaf ultrastructure and distribution of chlorenchyma in the two forms. *Ann. Bot.,* 51, 811-821.

Freitag, H. & Kadereit, G. (2014). C_3 and C_4 leaf anatomy types in Camphorosmeae (Camphorosmoideae, Chenopodiaceae). *Plant Systematics and Evolution*, 300, 665-687.

Hatch, M.D. (1976). Photosynthesis: the path of carbon. In: *Plant Biochemistry*, {eds. Bonner J. & Varner J.} Academic Press, New York. USA. pp. 797-844.

Hatch, M.D. (1987). C_4 photosynthesis: a unique blend of modified biochemistry, anatomy and ultrastructure. *Biochim. Biophys. Acta,* 895, 81-106.

Hattersley, P.W. (1984). Characterization of C_4 type leaf anatomy in grasses (Poaceae). M:BS area ratios. *Ann. Bot.*, 53, 163-180.

Hattersley, P.W. & Watson, L. (1975). Anatomical parameters for predicting photosynthetic pathways of grass leaves: the 'maximum lateral cell count' and the 'maximum cells distant count'. *Phytomorphology,* 25, 325-333.

542 Hattersley, P.W., Watson, L. & Osmond C.B. (1977). In situ immunofluorescent labelling of ribulose-
543 1, 5-bisphosphate Carboxylase in leaves of C_3 and C_4 plants. *Aust. J. Plant Physiol.*, 4, 523-539.
544
545 Heckmann, D., Schulze, S., Denton, A., Gowik, U., Westhoff, P., Weber, A.P.M., Lercher, M.J.
546 (2013) Predicting C_4 photosynthesis evolution: modular, individually adaptive steps on a Mount Fuji
547 fitness landscape. *Cell* 153, 1579-1588.
548
549 Khoshravesh, R., Lundsgaard-Nielsen. V., Sultmanis, S. & Sage, T.L. (2017). Light Microscopy,
550 Transmission Electron Microscopy, and Immunohistochemistry Protocols for Studying
551 Photorespiration. *Photorespiration*. Humana Press, New York, USA. pp. 243-270.
552
553 Kumar, D. & Kellogg, E. A. (2018). Getting closer: vein density in C_4 leaves. New Phytologist
554 (https://doi.org/10.1111/nph.15491)
555
556 Kümpers, M.C., Burgess, S.J., Reyna-Llorens, I., Smith-Unna, R., Boursnell, R., Hibberd, J.M.
557 (2017). Shared characteristics underpinning C_4 leaf maturation derived from analysis of multiple C_3
558 and C_4 species of *Flaveria*. *J. Exp. Bot*. 68, 177-189.
559
560 Li, Y., Xu, J., Haq, N.U., Zhang, H., Zhu, X.G. (2014) Was low CO_2 a driving force of C_4 evolution:
561 *Arabidopsis* responses to long-term low CO_2 stress. *J. Exp. Bot*., 65, 3657-3667.
562
563 Lundgren, M.R., Osborne, C.P. & Christin, P.A. (2014). Deconstructing Kranz anatomy to
564 understand C_4 evolution. *J. Exp. Bot*., 65, 3357-3369.
565
566 Lundgren, M.R. Besnard, G., Ripley, B.S., Lehmann, C.E.R., Chatelet, D.S., Kynast R.G., *et al.*
567 (2015). Photosynthetic innovation broadens the niche within a single species. *Ecol. Lett.*, 18, 1021-

1029.

Lundgren, M.R., Christin P.A., Gonzalez Escobar, E., Ripley, B.S., Besnard, G., Long, C.M., *et al.* (2016). Evolutionary implications of C_3-C_4 intermediates in the grass *Alloteropsis semialata*. *Plant Cell Environ.,* 39, 1974-1885.

McKown, A.D. & Dengler, N.G. (2007). Key innovations in the evolution of Kranz anatomy and C_4 vein pattern in *Flaveria* (Asteraceae). *Am. J. Bot.*, 94, 382-399.

McKown, A.D. & Dengler, N.G. (2009). Shifts in leaf vein density through accelerated vein formation in C_4 *Flaveria* (Asteraceae). *Ann. Bot*., 104, 1085-1098.

McKown, A.D., Cochard, H., Sack, L. (2010) Decoding leaf hydraulics with a spatially explicit model: principles of venation architecture and implications for its evolution. *Am. Nat*., 175, 447-460.

Nelson, T. (2011). The grass leaf developmental gradient as a platform for a systems understanding of the anatomical specialization of C_4 leaves. *J. Exp. Bot.,* 62, 3039-3048.

Nelson, T. & Langdale, J.A. (1989). Patterns of leaf development in C_4 plants. *Plant Cell*, 1, 3-13.

Olofsson, J.K. Bianconi, M., Besnard, G., Dunning, L.T., Lundgren, M.R., Holota, H., *et al*. (2016). Genome biogeography reveals the intraspecific spread of adaptive mutations for a complex trait. *Mol. Ecol.*, 25, 6107-6123.

Renvoize, S.A. (1987). A survey of leaf-blade anatomy in grasses XI. Paniceae. *Kew Bull.*, 42, 739-768.

Ripley, B.S., Cunniff, J. & Osborne, C.P. (2013). Photosynthetic acclimation and resource use by the C_3 and C_4 subspecies of *Alloteropsis semialata* in low CO_2 atmospheres. *Glob. Change Biol.*, 19, 900-910.

Sedelnikova, O.V., Hughes, T.E. & Langdale, J.A. (2018). Understanding the genetic basis of C_4 Kranz anatomy with a view to engineering C_3 crops. *Annual Review of Genetics*, 52 (https://doi.org/10.1146/annurev-genet-120417-031217).

Sage, R. F., Christin P.A., & Edwards E.J. (2011). The C_4 plant lineages of planet Earth. *J. Exp. Bot.*, 62, 3155-3169.

Sage, R.F., Khoshravesh, R., & Sage, T.L. (2014). From proto-Kranz to C_4 Kranz: building the bridge to C_4 photosynthesis. *J. Exp. Bot.*, 65, 3341-3356.

Scarpella, E., Barkoulas, M. & Tsiantis, M. (2010). Control of leaf and vein development by auxin. *CSH Perspect. Biol.*, 2, p.a001511.

Schlüter, U. & Weber, A.P. (2016). The road to C_4 photosynthesis: evolution of a complex trait via intermediary states. *Plant and Cell Physiology*, 57, 881-889.

Schneider, C.A., Rasband, W.S. & Eliceiri, K.W. (2012). NIH Image to ImageJ: 25 years of image analysis. *Nat. Methods*, 9, 671-675.

Scoffoni C. & Sack L. (2017) The causes and consequences of leaf hydraulic decline with dehydration. *J. Exp. Bot.*, 68, 4479-4496.

620

621 Scoffoni, C., Albuquerque, C., Broderson, C.R., Townes, S.V., John, G.P., Bartlett, M.K., Buckley,
622 T.N., McElrone, A.J., Sack, L. (2017a) Outside-xylem vulnerability, not xylem embolism, controls
623 leaf hydraulic decline during dehydration. *Plant Physiol.*, 173, 1197-1210.

624

625 Scoffoni, C., Albuquerque, C., Broderson, C.R., Townes, S.V., John, G.P., Cochard, H., Buckley,
626 T.N., McElrone, A.J., Sack, L. (2017b) Leaf vein xylem conduit diameter influences susceptibility to
627 embolism and hydraulic decline. *New Phytol*. 213, 1076-1092.

628

629 Soros, C.L. & Dengler, N.G. (2001). Ontogenetic derivation and cell differentiation in photosynthetic
630 tissues of C_3 and C_4 Cyperaceae. *American Journal of Botany*, 88, 992-1005.

631

632 Ueno, O. & Sentoku, N. (2006). Comparison of leaf structure and photosynthetic characteristics of
633 C_3 and C_4 *Alloteropsis semialata* subspecies. *Plant Cell Environ.*, 29, 257-268.

634

635 Venables, W.N. & Ripley, B.D. (2002). *Modern Applied Statistics with S.* 4th edition. Springer, New
636 York, USA.

637

638 von Caemmerer, S., Ghannoum, O., Pengelly, J.J. & Cousins, A.B. (2014). Carbon isotope
639 discrimination as a tool to explore C_4 photosynthesis. *J. Exp. Bot.*, 65, 3459-3470.

640

641 Wang, P., Khoshravesh, R., Karki, S., Tapia, R., Balahadia, C.P., Bandyopadhyay, A., *et al.* (2017).
642 Re-creation of a key step in the evolutionary switch from C_3 to C_4 leaf anatomy. *Curr. Biol.*, 27, 3278-
643 3287.

644

645 Watcharamongkol, T., Christin, P.A. & Osborne, C.P. (2018). C_4 photosynthesis evolved in warm

646 climates but promoted migration to cooler ones. *Ecology letters*, 21, 376-383.

647

648 Williams, B.P., Johnston, I.G., Covshoff, S., Hibberd, J.M. (2013) Phenotypic landscape inference
649 reveals multiple evolutionary paths to C_4 photosynthesis. *eLife* 2, e00961.

650

651 Wilson, J.T.R., Brown, R.H. & Windham, W.R. (1983). Influence of leaf anatomy on the dry matter
652 digestibility of C_3, C_4, and C_3/C_4 intermediate types of *Panicum* species. *Crop Sci.*, 23, 141-146.

TABLES

Table 1. Results of linear regression analyses on leaf components underlying M:BS in *Alloteropsis semialata*.

	F	DF	Adj R^2	*p*-value	*t*	*p*
Total M area / segment (μm²)	59.35	2, 47	0.704	1.38×10^{-13}		
Leaf thickness (μm)					3.98	0.00024
Interveinal distance[a] (μm)					10.58	5.07×10^{-14}
Interveinal distance[1] (μm)	343.4	2, 47	0.933	$< 2.2 \times 10^{-16}$		
Number M cells between veins[b]					25.48	$< 2 \times 10^{-16}$
M cell size (μm²)					6.97	9.22×10^{-9}
Total BS area / segment (μm²)	124.8	2, 47	0.835	$< 2.2 \times 10^{-16}$		
BS cell size[c] (μm²)					9.52	1.54×10^{-12}
Vein density (veins/segment)					4.23	0.00011

[a]Average distance between all veins; [b]Number of mesophyll (M) cells between all veins; [c]Cross-sectional area of inner bundle sheath (BS) cells on tertiary order veins.

Table 2. Coefficients of linear discriminants in a linear discriminant analysis on (top) five leaf anatomical traits expected to drive overall mesophyll to bundle sheath area ratios in *Alloteropsis semialata* and on (bottom) six leaf anatomical traits in 157 grass species, grouped as C_3 species, C_4 species using the inner sheath, and C_4 species using the outer sheath.

LDA on *Alloteropsis semialata* accessions		
Trait	*LD1*	*LD2*
Number of minor veins per segment	1.3591	0.3663
Number of mesophyll cells between major veins	-0.315	0.4881
Average area inner bundle sheath cell on tertiary veins (μm^2)	0.0123	-0.0104
Average area mesophyll cell (μm^2)	-0.0012	-7.82E-05
Leaf thickness (μm)	-5.52E-04	0.0189
LDA on 157 grass species + 1 C_3 and 1 C_4 *Alloteropsis semialata* accession		
Trait	*LD1*	*LD2*
proportion of veins that are minor	4.145779	-0.34605
outer BS cell width (μm)	-0.06433	0.080823
inner BS cell width (μm)	0.301257	0.004749
Leaf thickness (μm)	-0.0083	-0.00729
Mesophyll cell width (μm)	0.01989	-0.01048
Number of mesophyll cells between veins	-0.08007	-0.22237

FIGURE LEGENDS

Figure 1. Schematic of leaf anatomy and photosynthetic pathway in C_3, C_3-C_4, and C_4 grasses. In C_3 plants, CO_2 assimilation via the Calvin-Benson cycle (solid black circle) and CO_2 release via photorespiration (dashed black circle) both occur in mesophyll cells (light green). C_3 leaves consequently have larger areas of mesophyll tissue than bundle sheath tissue, where no photosynthetic activity occurs. C_3-C_4 plants use an intermediate physiology called C_2 photosynthesis, where the Calvin cycle occurs in mesophyll cells, like in C_3 plants. However, because glycine decarboxylase (GDC) is specifically localized to bundle sheath cells, the photorespiratory cycle is split across these two cell types, creating a weak CO_2-concentrating mechanism, where CO_2 is released in the bundle sheath and can be reassimilated via the Calvin cycle. C_2 photosynthesis therefore requires large areas of mesophyll for photosynthesis via an initial Calvin cycle, but also close contact between mesophyll and bundle sheath cells for the photorespiratory CO_2 pump. C_4 plants have a strong CO_2 concentrating mechanism whereby CO_2 is biochemically shuttled from the mesophyll into the bundle sheath. The high CO_2 concentration in the bundle sheath largely avoids oxygenation and thus, photorespiration. Photosynthesis via the C_4 cycle therefore requires large areas of bundle sheath tissue, but less mesophyll, which can be achieved via the insertion of minor veins. Dark blue, bundle sheath lacking chloroplasts; dark green, bundle sheaths with chloroplasts; light green, mesophyll cells; yellow, extraxylary fibers/bundle sheath extensions; grey, epidermal cells; light blue, veins; white, metaxylem.

Figure 2. Continuous variation in *Alloteropsis semialata* leaf anatomy, but distinct division among C_3, C_3-C_4, and C_4 types. Ratios of mesophyll (M) to bundle sheath (BS) area of individual accessions of C_3 (blue circles), C_3-C_4 (green circles), and C_4 (solid red circles) plants, ranked by M:BS value. n = 50. Lines delineating M:BS ratios that distinguish C_3 from C_3-C_4 (green) and C_3-C_4 from C_4 (red) are shown. For C_4 individuals, M:BS ratios are also calculated in the absence of minor veins (open red circles).

Figure 3. Linear discriminant analysis of leaf anatomical traits. The first (LD1) and second (LD2) dimensions of the LDA are plotted against each other with histograms of each dimension shown on the opposing axis for (A) the LDA on C_3, C_3-C_4, and C_4 *Alloteropsis semialata* accessions and (B) the LDA on 157 additional C_3, C_4 inner sheath, and C_4 outer sheath grass species. One C_3 and one C_4 *A. semialata* accession

were included this larger LDA and denoted by solid blue and red circles, respectively. Loading plots are overlaid via black arrows. M, mesophyll, IS, inner sheath; OS, outer sheath, nb.M, number of mesophyll cells between veins.

Figure 4. Diversity of intraspecific anatomical components. Histograms of (A) vein density (*i.e.*, the total number of veins per segment) and (B) the number of major veins per segment in C_4 (red; n=72) and non-C_4 (grey, n= 69) accessions. Scatter plots show (C) the average number of mesophyll (M) cells between major veins versus the average area of individual bundle sheath (BS) cells, with dot size scaled to the M:BS ratio, and (D) BS cell area versus outer sheath cell area, with dot size scaled to the number of veins per segment. Colors indicate photosynthetic type with C_3 (blue; n=17), C_3-C_4 (green; n=6), and C_4 (red; n=27).

FIGURES

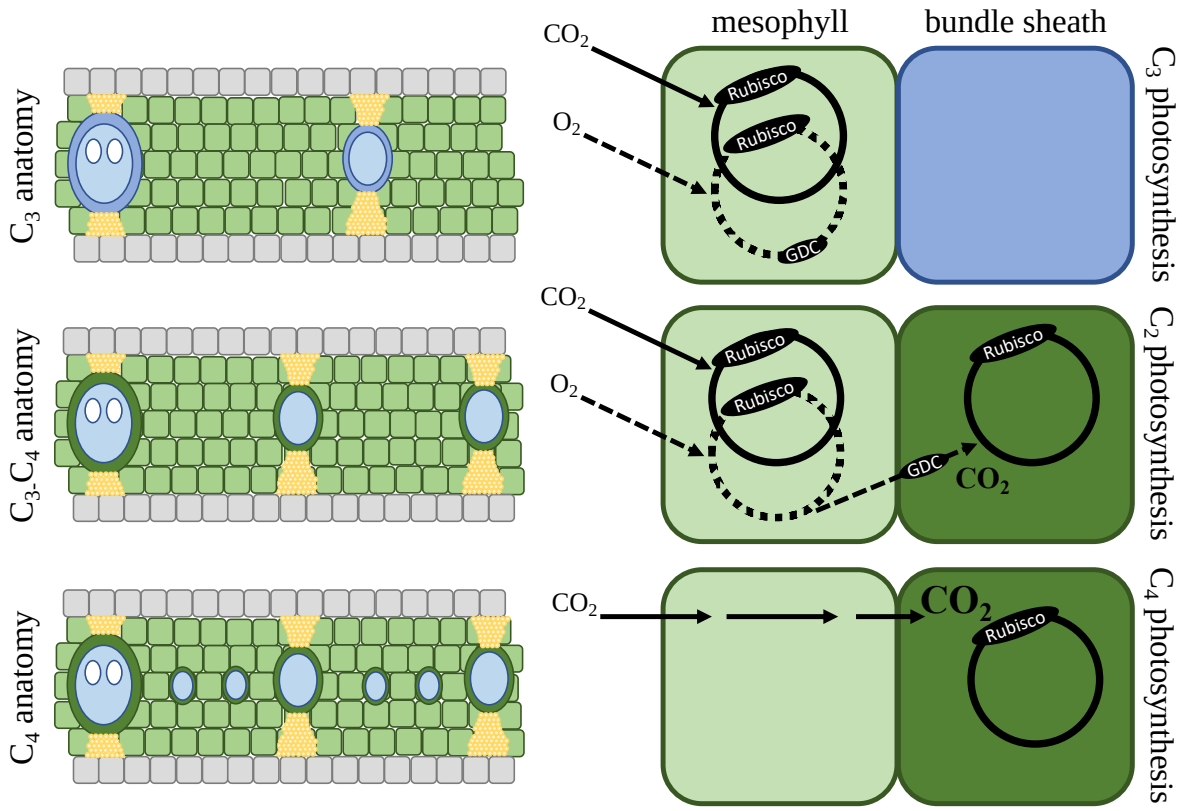

FIGURE 1

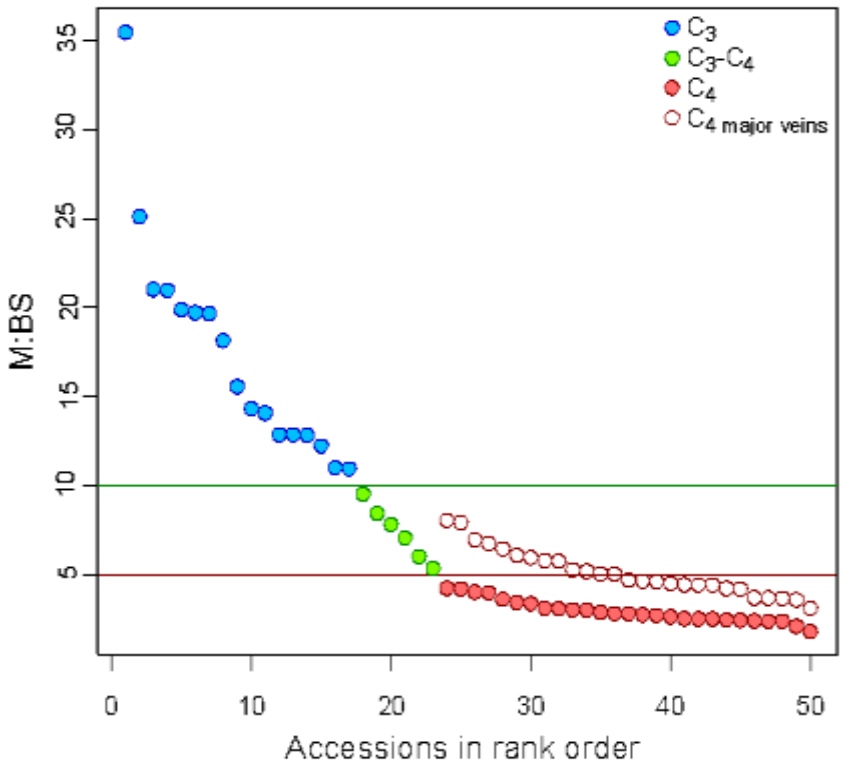

714

715 **FIGURE 2**

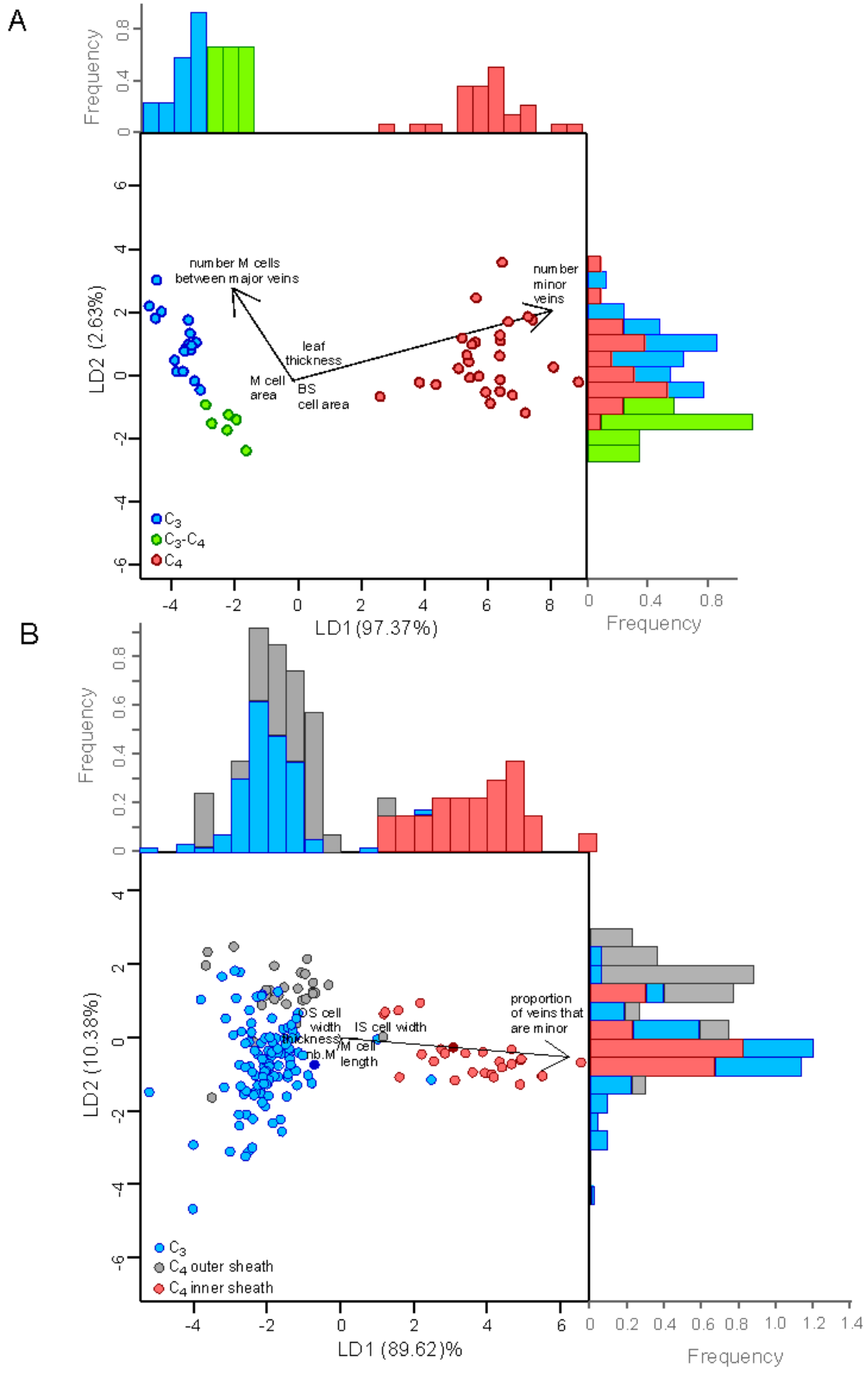

716

717 **FIGURE 3**

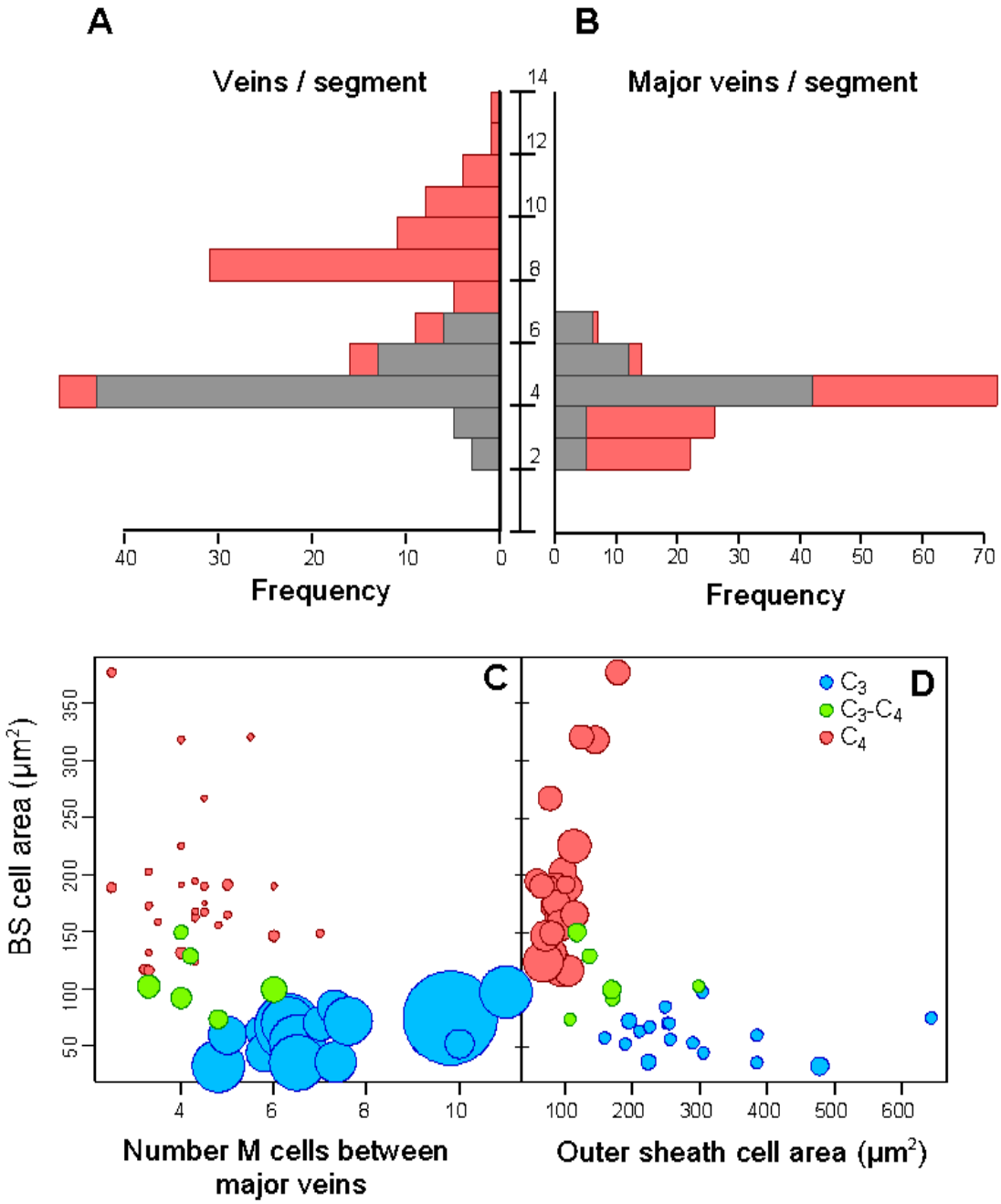

718

719

720

721 **FIGURE 4**

722

SUPPORTING INFORMATION

Supporting Information Materials 1. Ultrastructural characterization of C_3, C_3-C_4 and C_4 accessions

Dataset S1. Comprehensive anatomical measurements for all accessions

Dataset S2. Larger vein density dataset

Dataset S3. Field v controlled environment plasticity dataset

Dataset S4. Growth CO_2 concentration plasticity dataset

Figure S1. Example leaf anatomy measurement methods

Figure S2. Relationships between anatomical traits

Figure S3. Comparison of extraxylary fibre area in C_3, C_3-C_4 and C_4 accessions

Figure S4. Relationships between inner BS cell size and overall BS areas

Figure S5. Comparison of bundle sheath size in African and non-African C4 accessions.

Figure S6. Plasticity for leaf anatomical components by photosynthetic type

Figure S7. Organelle abundance differs between photosynthetic types.

Figure S8. Immunodetection of GLDH

Figure S9. Immunodetection of Rubisco large subunit

Table S1. Details used to determine photosynthetic pathway for accessions

Table S2. Details of the accessions used in the plasticity dataset